



# Release of deuterium from carbon–deuterium films on beryllium during carbide formation and oxidation

J. Roth <sup>a,\*</sup>, W.R. Wampler <sup>b</sup>, W. Jacob <sup>a</sup>

<sup>a</sup> Max-Planck-Institut für Plasmaphysik, Euratom Association, Boltzmannstraße 2, 85748 Garching, Germany

<sup>b</sup> Sandia National Laboratories, Albuquerque NM 87185-1056, USA

Received 6 June 1997; accepted 14 July 1997

## Abstract

Amorphous carbon–deuterium (a-C:D) films on beryllium substrates were vacuum annealed while the composition versus depth was followed using Rutherford backscattering, elastic recoil detection and Auger electron spectroscopy. The a-C:D film reacts with the Be substrate to form stoichiometric beryllium carbide, Be<sub>2</sub>C. The reaction begins at the interface and progresses through the film around 500°C until the entire film has reacted. D is absent from the reacted portion of the film but is still present in the unreacted carbon. The a-C:D films are removed from the Be without forming carbide by heating in oxygen at 400°C. Ion beam analysis was also used to study the oxidation of Be at temperatures up to 680°C. Through sequential exposures to different isotopes of oxygen it was shown that oxidation occurs by permeation of Be from the metal/oxide interface to the outer surface. © 1997 Elsevier Science B.V.

## 1. Introduction

In a thermonuclear fusion reactor, such as ITER [1], plasma facing materials will be eroded due to plasma ion and neutral bombardment. The present design for ITER uses carbon fiber composites (CFC) for the divertor plates and beryllium for the main plasma chamber walls [1]. Carbon eroded from the divertor plates will be deposited along with hydrogen isotopes from the plasma, onto less exposed areas including the Be wall of the main plasma chamber [2–4]. The inventory of tritium in this codeposited material could become large enough to restrict operation of the machine [5]. Methods to recover tritium from these codeposited layers are therefore of vital interest for the operation of ITER.

Previous studies have shown that deuterium is thermally desorbed from amorphous carbon–deuterium (a-C:D) films at temperatures above 600°C [6,7]. Oxidation in air removes the a-C:D layers at temperatures above 350°C

[7,8]. Heating in vacuum of a-C:D films on Be causes the release of D together with the formation of Be<sub>2</sub>C at temperatures above 500°C [9].

In the present paper, the interaction of Be with a-C:D films, the Be<sub>2</sub>C phase formation and the deuterium release are examined. Ion beam analysis is used to follow the evolution of the concentrations of Be, O, C and D and H versus depth in the near-surface region as the a-C:D layer reacts with the Be substrate. In addition, Auger electron spectroscopy (AES) gives information on the composition and chemical state of the surface. The oxidation kinetics of Be and a-C:D layers were also examined. From these studies a new picture emerges for the mechanism of deuterium release from a-C:D films on Be substrates.

## 2. Experimental

The samples were S65C grade vacuum hot pressed Be from Brush Wellman, Cleveland, Ohio, USA, with a composition of 99.5 wt% Be, 0.4 wt% O and 0.1 wt% other impurities, with 7.5 μm average grain size and with smooth polished surfaces. The a-C:D layers were deposited by

\* Corresponding author. Tel.: +49-89 3299 1387; fax: +49-89 3299 2591.

radio frequency plasma assisted chemical vapor deposition from a  $\text{CD}_4$  plasma [10]. The substrate temperature did not exceed  $50^\circ\text{C}$  during the deposition. Prior to deposition, the native oxide layer was reduced by in situ Ar plasma sputtering, such that the remaining BeO layer at the interface between the Be substrate and the a-C:D layer was less than 5 nm. At the surface of the a-C:D layer only small amounts of oxygen could be detected by AES after transfer through air to the analysis chamber. The a-C:D layer thicknesses were limited to less than 300 nm due to flaking of the films at larger thicknesses. Ion beam analysis, AES, thermal desorption and oxidation studies were performed in an UHV chamber attached to a 2.5 MeV ion accelerator at Sandia National Laboratories. The UHV chamber was equipped with detectors for Rutherford backscattering (RBS) and elastic-recoil detection (ERD) at scattering angles  $150^\circ$  and  $30^\circ$ , respectively. The depth profiles of Be, C and O were obtained by RBS and ERD gave the depth profiles of D and H. Analysis beams were  $^4\text{He}$  at 1.5 and 2.2 MeV for RBS and 2.5 MeV for ERD. The base pressure in the chamber was  $4 \times 10^{-10}$  mbar and did not exceed the  $10^{-10}$  mbar range during ion beam analysis. For in situ oxidation studies the chamber was backfilled to  $1.3 \times 10^{-5}$  mbar with  $^{18}\text{O}_2$ . The samples were radiatively heated by a W filament and the sample temperature was measured using an infrared thermometer.

In addition to in situ oxidation, a-C:D films on Be and Be samples without a-C:D films were also heated ex situ in a vacuum annealing furnace either in vacuum or in oxygen gas at 660 mbar. After ex situ heat treatment the samples were analyzed in a second ion beam analysis chamber, with detectors for RBS and ERD scattering angles of  $174^\circ$  and  $30^\circ$ , respectively.

### 3. Reaction of a-C:D layers with Be

The reaction of a-C:D layers with the Be substrate and its influence on the D desorption were studied by annealing samples in UHV stepwise at successively higher temperatures for 20 min at temperatures of 300, 400, 460, 483, 490 and  $560^\circ\text{C}$ . Samples were analyzed at room temperature after each anneal step. The RBS spectra in Fig. 1 show the transition from an a-C:D layer on Be to the fully reacted films in the temperature interval from 490 to  $560^\circ\text{C}$ . It can clearly be seen that the reaction begins at the interface and proceeds with increasing temperature farther into the carbon film. An oxide marker at the original interface remains at the interface between the Be substrate and the reacted film which indicates that the reaction occurs by Be diffusing from the metal through the oxide layer. In Fig. 2 the corresponding ERD spectra for deuterium are shown. It can be seen, that the deuterium profile becomes shallower as the thickness of the remaining unreacted a-C:D becomes smaller, while in the reacted layer the deuterium has been released. Fig. 3 shows the calculated depth profiles of O, C, Be and D from the combined RBS and ERD analysis for three different temperatures. For evaluating the depth profiles the program LORI [11] was used with cross sections for C, Be, O, D published in [12–15], respectively. The profiles show the saturated a-C:D films with a D/C ratio of about 0.4, a Be/C ratio of 2:1 in the reacted layer and the stationary 5 nm BeO layer at the interface. The Be/C ratio of 2:1 suggests the formation of a  $\text{Be}_2\text{C}$  phase. Indeed, examination of the carbon Auger line shows a transformation from a shape corresponding to graphitic carbon before annealing, to a shape corresponding to carbidic carbon after annealing at

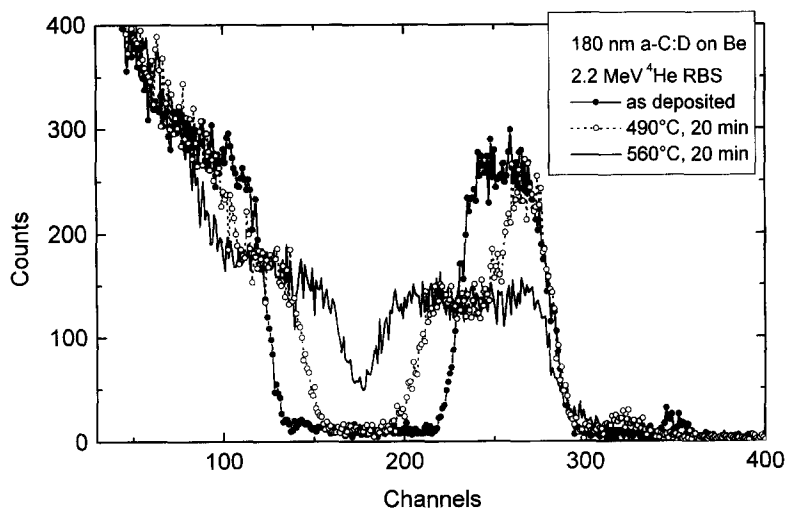


Fig. 1. RBS spectra of an a-C:D film on Be before and after annealing in vacuum.

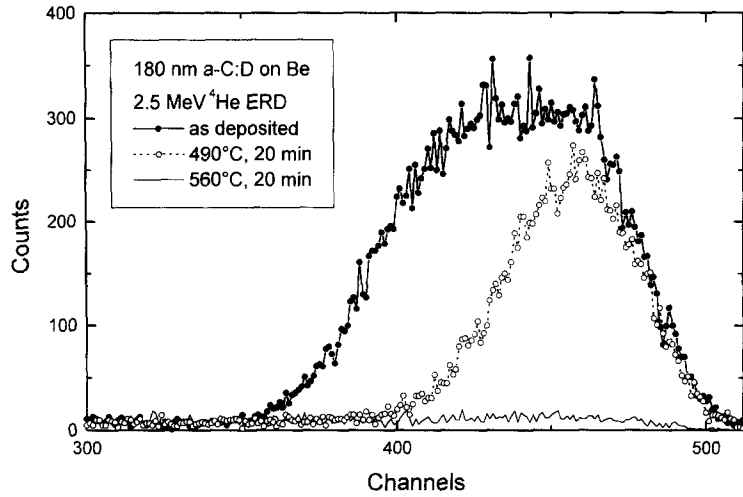


Fig. 2. ERD spectra of D in an a-C:D film on Be before and after annealing in vacuum.

temperatures where the film has completely reacted. Fig. 4 compares Auger spectra for pure Be covered with a native oxide, the deposited a-C:D layer and the fully reacted compound layer. RBS and AES show that a Be<sub>2</sub>C carbide has been formed.

In another experiment, a 100 nm thick Be layer was evaporated onto an isotropic fine grain graphite (ATJ)

substrate. This sample was annealed in vacuum at successively higher temperatures for 20 min at each temperature. RBS was used to monitor the near-surface composition versus depth after each anneal. There was no reaction between Be and carbon at temperatures up to 475°C. The Be mixed with the graphite substrate at temperatures of 500°C and higher. The observation that the Be–C reactions

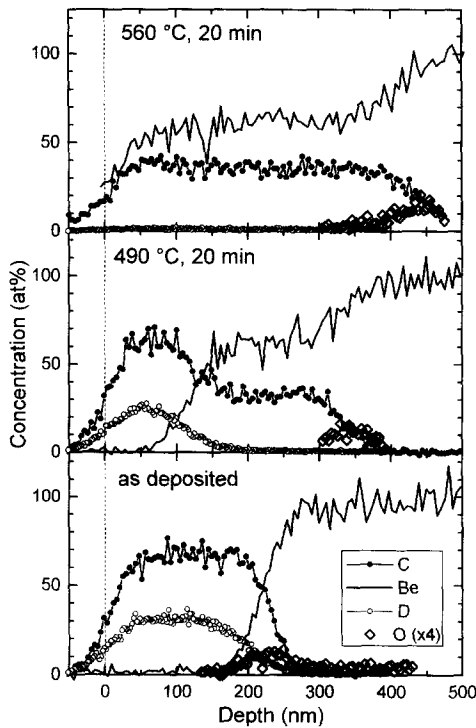


Fig. 3. Composition versus depth for a-C:D on Be before and after annealing, from RBS and ERD.

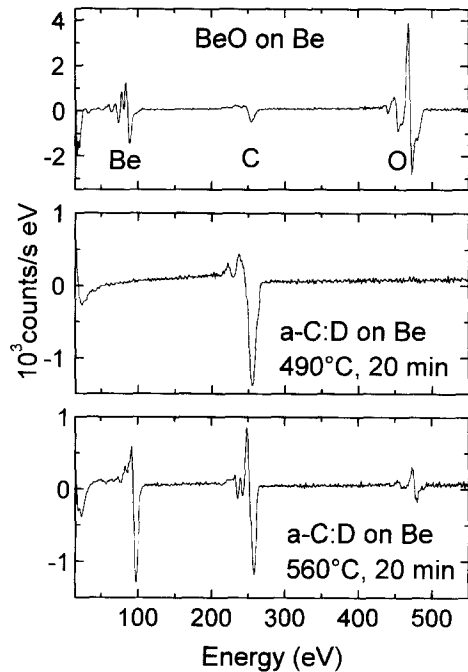


Fig. 4. AES spectra for an oxidized Be surface (top) and a-C:D on Be after vacuum annealing at 490°C (center) and 560°C (bottom). Peak positions are 88.7 eV for BeO (top) and 97.8 eV for Be<sub>2</sub>C (bottom).

occurred at close to the same temperature for Be on a graphite substrate and a-C:D on a Be substrate indicate that the reaction is not strongly affected by interfacial BeO layers.

#### 4. Oxidation of a-C:D

Removal of D from a-C:D layers on Be by oxidation was examined by annealing samples in oxygen gas in a separate vacuum furnace. The samples were exposed to 660 mbar O<sub>2</sub> for 1 h at temperatures between 350 and 425°C, thus below the temperature where the Be–C reaction occurred. Previous measurements of a-C:D layers on Si at these temperatures demonstrated the oxidative erosion of the a-C:D layers in air with simultaneous exchange of D by oxygen and hydrogen [8]. Fig. 5 shows the areal density of D and C remaining after annealing, as measured by ERD and RBS, for the films on Be substrates annealed in oxygen in the present study and for the films on Si substrates annealed in air from the previous study. Removal of the a-C:D film is very similar for the Be and Si substrates, since in both cases the film is removed at temperatures where the film has not chemically reacted with the substrate. Furthermore, it appears that water vapor in the air does not play a significant role in removal of the film or D, since the D release and film removal are the same for heating in air as for heating in pure oxygen. The depth profiles (Fig. 6) indicate that the release of D is accompanied by uptake of oxygen in the remaining layer.

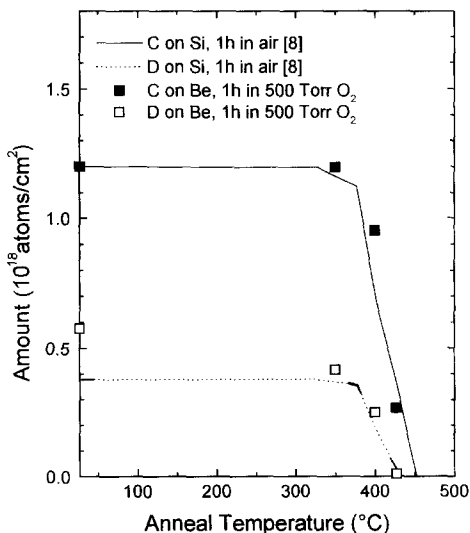


Fig. 5. Areal density of D and carbon remaining in a-C:D films on Be and Si substrates after 1 h isothermal anneals in air and oxygen versus anneal temperature.

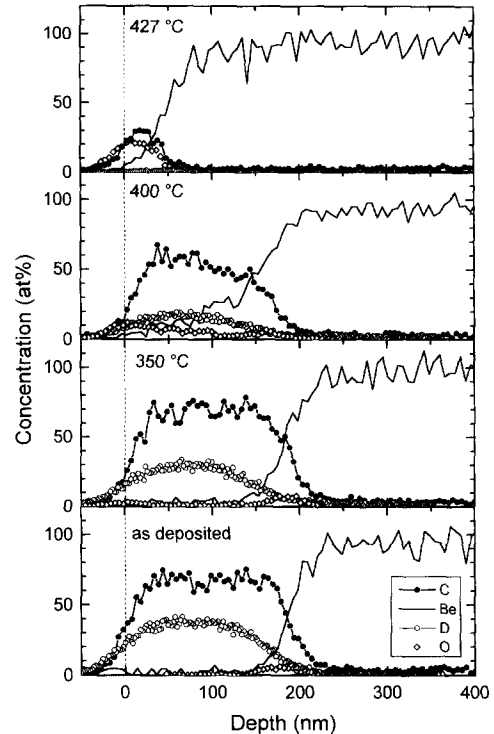


Fig. 6. Composition versus depth of an a-C:D film on Be after annealing in oxygen.

ERD showed that the deuterium release was not due to isotope exchange, i.e., displacement by hydrogen.

#### 5. Oxidation of Be

Gulbransen and Andrew [16] examined the kinetics of Be oxidation by measuring the weight gain with a vacuum microbalance. They observed that at constant temperature the oxidation proceeded with a parabolic time dependence. They also observed that the oxide growth rate depends strongly on temperature but only weakly on oxygen pressure. These observations indicate that diffusion of Be through the oxide is the rate determining process. A parabolic growth law is expected when growth occurs by bulk diffusion of Be through the oxide and sufficient oxygen is present to react all permeating Be to form new BeO at the surface. In this case, the permeating flux of Be and hence the BeO growth rate are inversely proportional to the BeO thickness:

$$dn/dt = D\Delta C/x = N_o dn/dt, \quad (1)$$

where  $x$  is the oxide thickness,  $n$  is the areal density of Be atoms in the BeO layer,  $N_o = 72.5/\text{nm}^3$  is the volume density of Be in the BeO layer,  $D$  is the diffusivity of the mobile Be atoms in BeO and  $\Delta C$  is the difference between the concentrations of mobile Be in the BeO at the

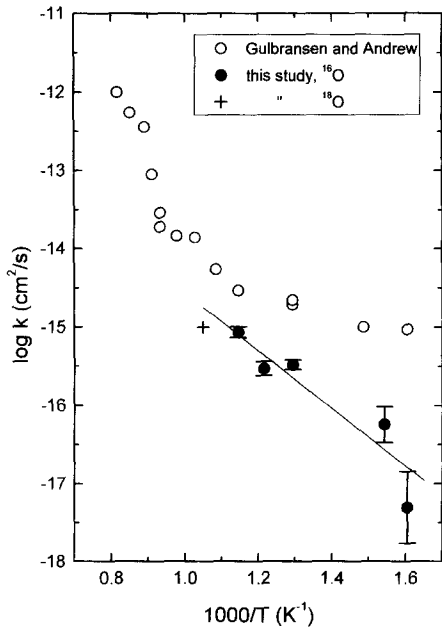


Fig. 7. Parabolic reaction rate coefficient for oxidation of Be metal in oxygen. The solid line indicates an activation energy  $Q = (0.73 \pm 0.14)$  eV.

metal/oxide interface and at the outer surface.  $\Delta C$  is assumed here to be independent of oxide thickness. Integrating Eq. (1) gives

$$x^2 = kt + x_0^2, \tag{2}$$

where  $k = 2D\Delta C/N_0$  is the rate constant and  $x_0$  is the initial oxide thickness at time  $t = 0$ .

The oxide thickness was measured by RBS on Be samples after heating in oxygen at a pressure of 660 mbar, typically for 1 h, at various temperatures. Heating temperatures and times as well as the resulting oxide thicknesses are given in Table 1. Parabolic growth kinetics was assumed and Eq. (2) was used to obtain a value for the rate constant  $k$  at each temperature. Fig. 7 shows an Arrhenius plot of the rate constants obtained in this way, together with those determined previously by Gulbransen and Andrew [16]. The fact that the earlier data for the rate

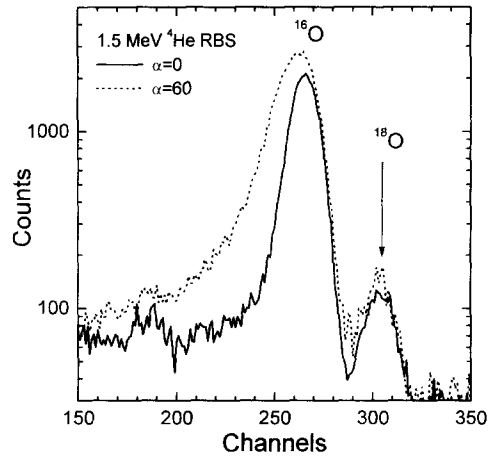


Fig. 8. RBS spectra of  $^{16}\text{O}$  and  $^{18}\text{O}$  in BeO on Be with the analysis beam at 0 (solid line) and 60 (dotted line) degrees from normal incidence.

constant are higher at low temperatures may be due to the less sensitive method of analysis by weight change compared to the ion beam analysis used in the present investigation. The present data show at temperatures below 680°C a decrease of the diffusion rate constant with an activation energy of  $0.73 \pm 0.14$  eV (Fig. 7).

Another experiment was done to confirm that new oxide forms at the external surface of the oxide, as expected when the rate controlling process is the permeation of Be through the oxide, and not at the Be/BeO interface due to permeation of O through the oxide. A Be sample was first oxidized by heating in the vacuum furnace to 600°C in  $^{16}\text{O}_2$  at 660 mbar for 2 h which produced a 25 nm thick oxide layer. The sample was then transferred into the UHV chamber and further oxidized at 680°C in  $^{18}\text{O}_2$  at a pressure of  $1.3 \times 10^{-5}$  mbar for 20 min. By using heavy oxygen, the new oxide can be discriminated from the previously existing oxide in the RBS spectra as shown in Fig. 8. An additional peak from  $^{18}\text{O}$  is observed and the energy of the peak shows that  $^{18}\text{O}$  is located on the surface and not at the interface. The absence of a shift in the energy of this peak when the sample is tilted relative to the analysis beam also shows that  $^{18}\text{O}$  is on the surface. This

Table 1  
Summary of experimental conditions and results for Be oxidation in 660 mbar oxygen

Anneal	Initial oxide thickness $x_0$ (nm)	Final oxide thickness $x$ (nm)	$k = (x^2 - x_0^2)/t$ ( $10^{-16}$ cm <sup>2</sup> /s)
$T$ (°C)	$t$ (s)		
–	no anneal	2.8	–
350	3600	2.8	0.077
375	3600	3.26	0.66
500	3600	5.85	3.35
550	3600	12.44	3.04
600	7200	2.8	24.95

result confirms that the oxide growth occurs by permeation of Be through the oxide and reaction at the surface and not by permeation of oxygen through the oxide to the Be/BeO interface.

## 6. Conclusions

The present investigations provide in situ depth analysis of the Be–C reaction and associated D release, combined with chemical phase analysis from AES lineshapes, for a-C:D films deposited on Be substrates. With this combination it could be shown that the a-C:D film reacts with the Be substrate to form stoichiometric beryllium carbide, Be<sub>2</sub>C. The reaction begins at the interface and progresses through the film around 500°C until the entire film has reacted. D is absent from the reacted portion of the film but is still present in the unreacted portion. Be is the diffusing species as seen from an oxide marker at the interface.

Our measurements of oxide growth on Be metal give values for the oxidation rate constant which are slightly lower than those reported in an earlier study [16]. Through the use of different oxygen isotopes we have shown that the new oxide forms at the outer surface of the BeO, demonstrating that the oxidation occurs by diffusion of Be atoms through the oxide to the outer surface.

## Acknowledgements

Sandia is a multiprogram laboratory operated by Sandia Corporation, a Lockheed Martin Company, for the United States Department of Energy under Contract DE-ACO4-94AL85000.

## References

- [1] R. Parker, G. Janeschitz, H. Pacher, D. Post, S. Chiochio, G. Federici, P. Ladd, *J. Nucl. Mater.* 241–243 (1997) 1.
- [2] W.R. Wampler, B.L. Doyle, S.R. Lee, A.E. Pontau, B.E. Mills, R.A. Causey, D. Buchenauer, H.F. Dylla, M.A. Ulrickson, P.H. LaMarche, *J. Vac. Sci. Technol. A6* (1988) 2111.
- [3] C.H. Skinner, W. Blanchard, J. Kamperschroer, P. LaMarche, D. Mueller, A. Nagy, S. Scott, G. Ascione, E. Amarescu, R. Camp, M. Casey, J. Collins, M. Cropper, C. Gentile, M. Gibson, J. Hosea, M. Kalish, J. Langford, S. Langish, R. Mika, D.K. Owens, G. Pearson, S. Raftopoulos, R. Raucci, T. Stevenson, A. Von Halle, D. Voorhees, T. Walters, J. Winston, *J. Vac. Sci. Technol. A14* (1996) 3267.
- [4] J.P. Coad, *J. Nucl. Mater.* 226 (1995) 156.
- [5] G. Federici, C.H. Wu, *J. Nucl. Mater.* 207 (1993) 62.
- [6] B.L. Doyle, W.R. Wampler, D.K. Brice, *J. Nucl. Mater.* 103&104 (1981) 513.
- [7] R.A. Causey, W.R. Wampler, D. Walsh, *J. Nucl. Mater.* 176&177 (1990) 987.
- [8] W. Wang, W. Jacob, J. Roth, *J. Nucl. Mater.* 245 (1997) 66.
- [9] K. Ashida, K. Watanabe, T. Okabe, *J. Nucl. Mater.* 241 (1997) 1060.
- [10] A. Annen, R. Beckmann, W. Jacob, *J. Non-Cryst. Solids* 209 (1997) 240.
- [11] P. Borgesen, B.M.U. Scherzer, R. Behrisch, L.G. Svendsen, S.S. Eskildsen, Computer program for the evaluation of ion beam analysis energy spectra, Max-Planck Institut für Plasmaphysik, Garching, Report IPP 9/42 (1983).
- [12] Y. Feng, Z. Zhou, Y. Zhou, G. Zhao, *Nucl. Instrum. Meth.* B86 (1994) 225.
- [13] J. Liu, Z. Zheng, W.-K. Chu, *Nucl. Instrum. Meth.* B108 (1996) 247.
- [14] Z.Y. Zhou, Y.Y. Zhou, Y. Zhang, W.D. Xu, G.Q. Zhao, J.Y. Tang, F.J. Yang, *Nucl. Instrum. Meth.* B100 (1995) 524.
- [15] F. Besenbacher, I. Stensgaard, P. Vase, *Nucl. Instrum. Meth.* B15 (1986) 459.
- [16] E.A. Gulbransen, K.F. Andrew, *J. Electrochem. Soc.* 97 (1960) 383.